$F^{19}(He^3,He^3)F^{19}$ and $F^{19}(He^3,\alpha)F^{18}$ Reactions and States in F^{18} at 3.06 and 3.13 MeV

G. M. Matous,*† G. H. Herling, and E. A. Wolicki
Nuclear Physics Division, U. S. Naval Research Laboratory, Washington, D. C.
(Received 26 July 1966)

Differential cross sections have been obtained for the elastic scattering of He^3 from F^{19} at 4.0, 6.0, and 8.0 MeV. The results obtained at 6.0 and 8.0 MeV were fitted using optical potentials. Measurements on the $F^{19}(He^3,\alpha)F^{18}$ reaction were made on resolved alpha-particle groups leading to states in F^{18} at 3.06 and 3.13 MeV. Excitation functions were obtained in the incident energy range from 4.0 to 10.1 MeV at laboratory angles of 20°, 50°, 130°, and 170°. Differential cross sections as a function of angle were obtained at 4.0, 6.0, and 8.0 MeV. Zero-range distorted-wave Born-approximation calculations were made assuming pickup as the dominant mechanism. The 3.13-MeV level in F^{18} has been assigned a negative parity, that at 3.06 MeV has been assigned a positive parity. The ratio of spectroscopic factors obtained for these two levels is approximately equal to 1.

I. INTRODUCTION

NUCLEI with $A=18$ have recently been receiving much theoretical and experimental attention.[1–9] The observations of low-lying states exhibiting collective properties[6] and negative parity states[7] have shown that the low-energy spectra of several nuclei in the $(2s1d)$ shell may not be described simply in terms of the extra-core particles interacting with each other and with a spherical, inert O^{16} core. Considerable evidence exists to show that nuclei with $A=19$ and $A=20$ exhibit collective properties.[10–12] For the mass-18 nuclei, O^{18}, F^{18}, and Ne^{18}, however, detailed comparisons between theoretical calculations and observed nuclear properties are hampered by the lack of data. While a number of the levels of F^{18} with excitation energies below 3.5 MeV have been assigned to states belonging to the $(2s1d)^2$ configuration,[1,9] there are a number of others which have not been so identified. Level parameter assignments are needed for F^{18} not only to identify those states which are isobaric analogs of states in O^{18}, for which recent calculations have shown that the $(1p)^{-1}(2s1d)^3$ configuration[3] and the $(1p)^{-2}(2s1d)^4$ configuration[5] can lead to low-lying states, but also to assist in the spectroscopic classification of those states which belong to the $T=0$ spectrum of the mass-18 system.

A second area of interest is that of investigating, at low energies, the utility of the (He^3,α) reaction for obtaining spectroscopic information about energy levels in light nuclei. At higher energies and on medium-weight nuclei, a number of investigations have shown that the (He^3,α) reaction proceeds directly and can be used to obtain such information.[13,14] For light nuclei and energies below 10 MeV, some questions exist with regard to the applicability of both the optical model for strongly absorbed particles such as He^3 and He^4 and the distorted-wave Born-approximation (DWBA) calculations for (He^3,α) reactions using the zero-range approximation. The $F^{19}(He^3,\alpha)F^{18}$ reaction leading to the 3.063- and the 3.133-MeV levels in F^{18} was judged to be a favorable case for studying questions about the (He^3,α) reactions as well as for providing needed spectroscopic information. The close spacing of these levels was expected to minimize the effects of differing alpha-particle energies on the optical model and DWBA analysis.

The level at 3.063 MeV had been assigned a spin of either 1, 2, or 3 by Poletti and Warburton.[9] Recently, Olness and Warburton[15] have assigned a spin of 2 to this level. Previous work by Matous and Browne[8] had shown that the $Ne^{20}(d,\alpha)F^{18}$ reaction populated both the 3.133-MeV and the 3.063-MeV levels, in a ratio of 2 to 1. Since the 3.063-MeV level is thought to be the isobaric spin-analog state of the first excited $J^\pi=2^+$, $T=1$ state at 1.982 MeV in O^{18}, their results showed that some violation of the isobaric spin-selection rule was occurring, and that possibly the 3.063-MeV state had an appreciable mixture of $T=0$. At the time this experiment was started, neither the spin nor the parity of the 3.133-MeV level was known. These quantities were needed to determine if possibly the isobaric spin mixing

* National Academy of Sciences—National Research Council Postdoctoral Resident Research Associate–NRL.
† Present address: College of the Holy Cross, Worcester, Massachusetts.
[1] B. H. Flowers and D. Wilmore, Proc. Phys. Soc. (London) **83**, 683 (1964).
[2] J. P. Elliott and M. Harvey, Proc. Roy. Soc. (London) **A272**, 557 (1963).
[3] M. Harvey, Phys. Letters **3**, 209 (1963).
[4] M. de Llano, P. A. Mello, E. Chacon, and J. Flores, Nucl. Phys. **72**, 379 (1965).
[5] T. Engeland, Nucl. Phys. **72**, 68 (1965).
[6] A. E. Litherland, M. J. L. Yates, B. M. Hinds, and D. Eccleshall, Nucl. Phys. **44**, 220 (1963).
[7] A. A. Jaffe, F. De S. Barros, P. D. Forsyth, J. Muto, I. J. Taylor, and S. Ramavataram, Proc. Phys. Soc. (London) **76**, 914 (1960).
[8] G. M. Matous and C. P. Browne, Phys. Rev. **136**, B399 (1964).
[9] A. R. Poletti and E. K. Warburton, Phys. Rev. **137**, B595 (1965).
[10] J. D. Prentice, N. W. Gebbie, and H. S. Caplan, Phys. Letters **3**, 201 (1963).
[11] A. E. Litherland, M. A. Clark, and C. Broude, Phys. Letters **3**, 204 (1963).
[12] A. E. Litherland, J. A. Kuehner, H. E. Gove, M. A. Clark, and E. Almquist, Phys. Rev. Letters **7**, 98 (1961).
[13] A. G. Blair and H. E. Wegner, Phys. Rev. **127**, 1233 (1962).
[14] D. Cline, W. P. Alford, and L. M. Blau, Nucl. Phys. **73**, 33 (1965).
[15] J. W. Olness and E. K. Warburton, Bull. Am. Phys. Soc. **11**, 405 (1966).

was occurring between the 3.063- and the 3.133-MeV levels. Subsequently a spin assignment of 1 was made to this level,[9] but the parity was not determined.

II. EXPERIMENTAL PROCEDURE AND RESULTS

The NRL 5-MV Van de Graaff accelerator was used to provide beams of He^3 particles in the energy range from 4.0 to 10.1 MeV. The beam was magnetically analyzed before striking the target. Measurements were made in the horizontal plane on He^3 particles scattered elastically from F^{19} and Ca^{40} nuclei, and on alpha particles from the $F^{19}(He^3,\alpha)F^{18}$ reaction. Most of the measurements on elastic scattering were performed in an 18-in. internal diameter scattering chamber which contains four independently movable, detector-positioning arms. The emitted charged particles were detected with surface-barrier solid-state detectors, the output pulses of which were sent into a multichannel pulse-height analyzer. For the $F^{19}(He^3,\alpha)F^{18}$ reaction, most of the measurements were made with a 180-deg deflection, 20-in. radius, double-focusing, magnetic spectrometer. A 30 mm long by 15 mm wide position sensitive detector, located in the image plane of the spectrometer, was used to detect the analyzed particles. The 30-mm length corresponded to a 2% energy change along the image plane.

The targets consisted of thin films of CaF_2 which were evaporated onto thin carbon foils. The surface density of the CaF_2 targets ranged from 10 to 50 μg cm^{-2}; the carbon foils generally had a surface density of 20 μg cm^{-2} or less. These targets were sufficiently thin so that the alpha-particle groups under study, i.e., those leaving the residual F^{18} nucleus in the 3.063- and 3.133-MeV levels, could be resolved. These two alpha-particle groups will be designated herein as α_8 and α_9, respectively.

For the $F^{19}(He^3,\alpha)F^{18}$ reaction, the center-of-mass motion causes the alpha-particle energy to change relatively rapidly with laboratory angle. At 8.0 MeV He^3 energy and at 90°, for example, the energy of α_8 is changing by 54 keV/deg. Because of this large kinematic effect, it was generally necessary, in order to resolve α_8 from α_9, to restrict the angle subtended at the target by the detector to values smaller than 1 deg. In order to optimize the yield while keeping the alpha groups resolved, it was necessary to adjust target thickness and geometry in several steps as the incident energy was increased. Target thickness was the more important factor at low energies, and subtended angle was the more important at high energies. Figure 1 shows the resolved alpha groups at 4.0-MeV incident energy and 20° laboratory angle as obtained with the magnetic spectrometer and the position sensitive detector.

Excitation functions were obtained by normalizing the observed yields at each energy to the corresponding integrated beam charge. Angular distributions were obtained by normalizing the observed yield at each angle to the corresponding yield observed in a fixed monitor detector, thus taking into account target nonuniformities. Relative detector solid angles were measured either by using a radioactive alpha-particle source placed at the same location as the beam spot on target or by measuring the elastic scattering yields from the $Ca^{40}(He^3,He^3)Ca^{40}$ reaction at 30° for each detector.

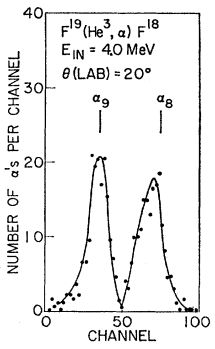

FIG. 1. Position pulse-height spectrum of groups α_8 and α_9 detected at the output of a magnetic spectrometer with a position sensitive solid-state detector.

The stability of the CaF_2 targets under bombardment, and the ratio of particle yields due to F^{19} to those due to Ca^{40} were checked and found to be constant to within a few percent.

The yield from the $Ca^{40}(He^3,He^3)Ca^{40}$ reaction was used to obtain absolute normalizations of all of the $F^{19}(He^3,He^3)F^{19}$ and $F^{19}(He^3,\alpha)F^{18}$ reaction data. The $Ca^{40}(He^3,He^3)Ca^{40}$ reaction was assumed to proceed by pure Rutherford scattering at 30° and 4.0-MeV incident energy. Measurements on this reaction at 25° and 20° at 4.0 MeV, and at 30° at 6.0- and 8.0-MeV incident energy were all consistent with this assumption.

The angular distributions of elastically scattered He^3 particles from F^{19} were measured at 4.0, 6.0, and 8.0 MeV using solid state detectors. At angles greater than 30°, the elastic scattering peaks due to C^{12}, O^{16}, F^{19}, and Ca^{40} were well resvoled. For angles of 30° and smaller, measurements were made with the magnetic spectrometer in order to subtract a small contribution due to O^{16} from the F^{19} yield. These data are shown in Fig. 2.

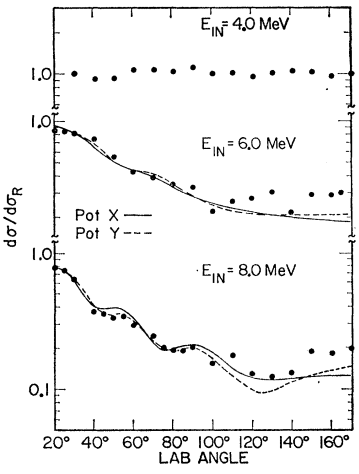

FIG. 2. Measured $d\sigma/d\sigma_R$ (dots) for the $F^{19}(He^3,He^3)F^{19}$ reaction at 4.0-, 6.0-, and 8.0-MeV incident energy. The full and dashed curves are optical-potential fits using potentials X and Y, respectively.

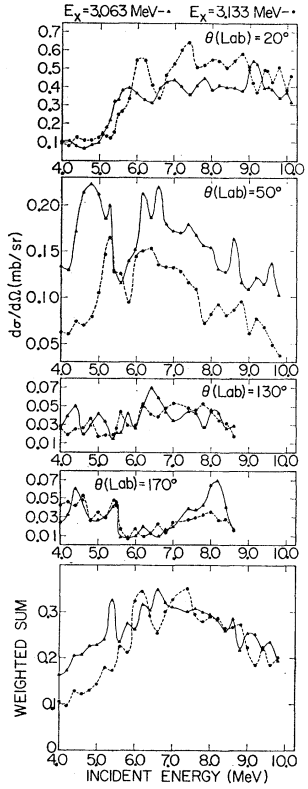

FIG. 3. Excitation functions for the $F^{19}(He^3,\alpha)F^{18}$ reaction for incident energies from 4.0 to 10.1 MeV. The solid and dashed lines drawn through the experimental points correspond to alpha groups leaving F^{18} in the 3.063- and 3.133-MeV levels, respectively. The topmost four graphs show the data obtained at 20°, 50°, 130°, and 170° in the laboratory system. The bottom graph shows the sum, weighted by $\sin\theta$, of the measured differential cross sections for these four angles.

For angles smaller than 100°, the errors in the measurements of the differential cross sections for elastic scattering are estimated to be smaller than $\pm 5\%$.

$F^{19}(He^3,\alpha)F^{18}$ excitation functions for α_8 and α_9 were measured from 4.0 to 10.1 MeV at laboratory angles of 20°, 50°, 130°, and 170°. The results are shown in Fig. 3. For these, a monitor was not practical, and it was necessary to rely on beam current integration. The target was checked periodically for stability by measuring the reaction yield at 4.0 MeV. There was no measurable change in the amount of CaF_2 on the target during the runs.

Differential cross sections for α_8 and α_9 were measured at 4.0, 6.0, and 8.0 MeV, in the laboratory angular range from 3° to 170°. These data are presented in Figs. 4 and 5. For angles smaller than 100°, the uncertainties in the data are estimated to be less than 5%, while for angles greater than 100°, the uncertainties are less than 20%. The excitation function for each angle was normalized at one energy and then checked for consistency with the value obtained for that angle from the angular distributions at the other energies. In general, the agreement was found to be within statistics.

III. ELASTIC SCATTERING

The $F^{19}(He^3,He^3)F^{19}$ elastic scattering data at 6.0- and 8.0-MeV incident energy were fitted using the automatic search program ABACUS[16] and an optical potential of the form

$$U(r)=-V\{1+\exp[(r-r_0A^{1/3})/a]\}^{-1} -iW\{1+\exp[(r-r_0'A^{1/3})/a']\}^{-1}. \quad (1)$$

Preliminary calculations made with the range and diffuseness parameters the same for both the real and imaginary parts of the potential did not produce satisfactory fits to the elastic scattering. Moreover, with such potentials for the incident channel, it was not possible to fit the reaction angular distributions for α_8 and α_9 with a single potential for the exit channel. A potential was then adopted for which the range and diffuseness parameters were different for the real and imaginary parts. Yntema, Zeidman, and Bassel[17] had previously used this form, and found that the potential which best fit the elastic scattering angular distributions of 12-MeV He^3 particles from a number of nuclei in the range from $A=20$ to $A=90$ had a relatively weak but long-range imaginary term. For all of the nuclei studied, the following values of the geometrical parameters were obtained: $r_0=1.07$ F, $a=0.754$ F, $r_0'=1.81$ F, and $a'=0.592$ F. In the present work, searching was performed on these parameters as well as on V and W. Starting points were chosen to have the imaginary radius parameter larger than the real. The real part of the potential was allowed to vary in the range from 100 to 210 MeV. This range was chosen because of evidence from a number of analyses of experiments[18–21] that the He^3 potential should be equal to approximately three times the single-nucleon potential. Furthermore, Alford, Blau, and Cline[14] found that in order to fit their results for the $Ca^{40}(He^3,\alpha)Ca^{39}$ reaction with a DWBA calculation, a real potential depth for He^3 of about 180 MeV was required.

For the searches at 6.0 MeV, the geometrical parameters were constrained to the values obtained at 8.0 MeV. In the course of searching, it was found that the geometrical parameters which had been used by Siemssen to fit the elastic scattering of He^3 from F^{19} at 9.0 MeV[20] also were very close to the optimum parameters found in the present work for 8.0 MeV. The geometrical parameters were then fixed at the values found at 9.0 MeV and the remaining searching was performed on V and W. It is interesting to note that the values used for r_0' and a' are identical with those used in Ref. 17 for the scattering of 12.0-MeV He^3 particles from a number of nuclei.

The elastic scattering data obtained at 4.0, 6.0, and 8.0 MeV, and the optical-potential fits for the two

[16] E. H. Auerbach (unpublished).

[17] J. L. Yntema, B. Zeidman, and R. H. Bassel, Phys. Letters **11**, 302 (1964).

[18] W. Parker Alford, L. M. Blau, and D. Cline, University of Rochester Report No. UR-875-65 (unpublished).

[19] R. H. Siemssen, T. H. Braid, D. Dehnhard, and B. Zeidman, Phys. Letters **18**, 155 (1965).

[20] R. H. Siemssen, L. L. Lee, Jr., and D. Cline, Phys. Rev. **140**, B1258 (1965).

[21] E. R. Flynn and R. H. Bassel, Phys. Rev. Letters **15**, 168 (1965).

higher energies are shown in Fig. 2, and the corresponding parameters are given in Table I. With the geometrical parameters held fixed, χ^2 minima were found for two sets of V and W at each He^3 energy. A comparison of the wave functions and phase shifts corresponding to the two potentials showed that they are related by the well-known half-wavelength ambiguity.[22,23]

IV. DISTORTED-WAVE ANALYSIS AND DISCUSSION

Distorted-wave Born-approximation pickup calculations were performed with the Oak Ridge code JULIE.[24] The forward peaking of the angular distributions, especially at 8.0 MeV, suggests that pickup is the dominant reaction mechanism. The excitation functions of Fig. 3 are fairly smooth for energies greater than 6.5 MeV, but they have a pronounced structure in the neighborhood of 6.0 MeV. Nevertheless, the quantity

$$\tilde{\sigma}(E)=\sum_{i=1}^{4}\frac{d\sigma}{d\Omega}(E,\theta_i)\sin\theta_i \qquad (2)$$

is a slowly varying function, and the energy dependence favors a direct process. The DWBA calculations have yielded consistent results at both energies; however, the analysis at 6.0 MeV was not as satisfactory as that at 8.0 MeV.

Entrance-Channel Optical Potential

Potentials X and Y, obtained from the He^3 elastic scattering analyses and listed in Table I, were both employed in the DWBA calculations.

Exit-Channel Optical Potential

It is not possible to obtain elastic scattering data for the exit channel because the F^{18} nucleus is short lived. To the extent that the optical potential for a given projectile is a slowly varying function of incident energy and target nucleus, extrapolation or interpolation of parameters may be attempted. However, analyses of scattering of 24.7-MeV alpha particles from a number of nuclei have failed to yield an optical potential which has a simple, smooth variation with mass number.[25] The exit-channel parameters V, W, $r_0=r_0'$, $a=a'$, therefore, were systematically scanned in order to fit the reaction angular distributions. Independent scans were performed for both He^3 potentials, which, although equivalent for elastic scattering, are not accompanied by similarly equivalent alpha-particle potentials in the calculations of this paper.

[22] R. M. Drisko, G. R. Satchler, and R. H. Bassel, Phys. Letters 5, 347 (1963).
[23] C. M. Perey and F. G. Perey, Phys. Rev. 132, 755 (1963).
[24] R. M. Drisko (unpublished).
[25] L. McFadden and G. R. Satchler, Nucl. Phys. 84, 177 (1966).

TABLE I. Optical potential parameters employed in the DWBA calculations for the $F^{19}(He^3,\alpha)F^{18}$ reaction at 6.0 and 8.0 MeV.

	$E_{in}(He^3)$	6.0 MeV	8.0 MeV
	Entrance channel		
	$r_0=1.05$ F, $a=0.829$ F	$r_0'=1.81$ F, $a'=0.592$ F	
Pot. X	V (MeV)	201.55	183.31
	W (MeV)	25.90	23.23
Pot. Y	V (MeV)	153.22	141.02
	W (MeV)	15.95	16.00
	Exit channel		
Pot. X	V (MeV)	60.00	65.00
	W (MeV)	10.25	16.50
	r_0 (F)	1.58	1.58
	a (F)	0.52	0.52
Pot. Y	V (MeV)	39.00	35.00
	W (MeV)	5.00	12.25
	r_0 (F)	1.45	1.45
	a (F)	0.51	0.51

Plausible ranges for the parameters were obtained from Ref. 25. A bias in favor of "small-V" potentials was introduced because of the suggestion that such alpha-particle potentials may be preferred for light nuclei.[25] With $r_0=1.75$ F, and $a=0.5$ F, the parameters V and W were varied over the region ($20\leq V\leq 80$ MeV, $2\leq W\leq 22$ MeV) in an attempt to fit the α_8 angular distribution at an incident energy of 8.0 MeV. The several pairs of values (V,W) which yielded qualitatively superior fits were then employed for a scan of the region ($1.25\leq r_0\leq 1.90$ F, $0.30\leq a\leq 0.60$ F), and the results were compared with the 8.0-MeV α_9 data. The best quadruplets (V,W,r_0,a) thus obtained supplied starting points for small simultaneous variations of the four parameters in order to obtain a best fit for the forward angles of the α_9 differential cross section. These final best-fit potentials were then utilized in single calculations for comparison with the 8.0-MeV α_8 angular distribution. The calculations for 6.0-MeV incident energy were performed with the geometrical parameters obtained at 8.0 MeV. The α_9 data were fitted by allowing V and W to vary, and the best-fit quadruplets served as the alpha-particle potential parameters in the calculations for α_8 at 6.0 MeV.

Although the results for α_9, which are shown in Fig. 5, are the best fits to these angular distributions, fits for α_8 which are better than those shown in Fig. 4 were obtainable, as one would expect, if all four parameters were allowed to vary not only with the incident energy but also with the state of the residual nucleus. Because the energy difference of the two groups of alpha particles leaving F^{18} in the 3.063- and 3.133-MeV excited states is small, the usual energy-dependent effects on optical potentials were expected to be small, and the identity of the potentials for the two alpha groups was explicitly required. The same procedure for the alpha-particle potential was followed for both sets of He^3 potentials, and the optical-model parameters for the final calculations are presented in Table I.

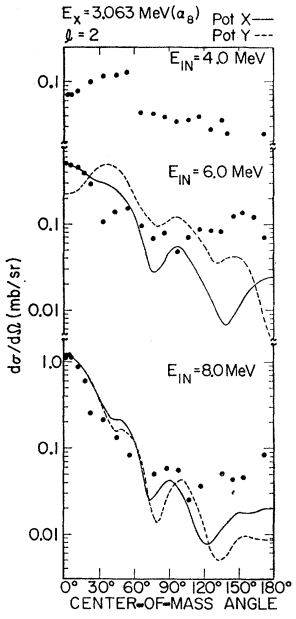

FIG. 4. Measured differential cross sections (dots) for the $F^{19}(He^3,\alpha_8)F^{18}$ reaction at 4.0-, 6.0-, and 8.0-MeV incident energy. The full and dashed curves are zero-range DWBA fits to the data for potential sets X and Y, respectively.

Form Factor

The form factor was chosen to be an eigenstate of a central Saxon well with $r_0=1.20$ F, $a=0.65$ F, and a depth which was adjusted so as to yield an eigenenergy determined according to the separation energy prescription. Because there is more than one nucleon outside of the O^{16} core, the form factor may differ, at distances smaller than the nuclear radius, from that which was employed; however, the exponential tail of the radial function is correct.[26,27] Although adjustments of the form-factor parameters or the employment of cutoff radii might provide partial compensation for this effect, such calculations were not attempted because the possible improvement in fit would seem to be offset by a loss of definiteness.

The 3.063-MeV Level

The angular distributions of alpha particles leaving F^{18} in the 3.063-MeV excited state are shown in Fig. 4. The solid and broken curves are the results of DWBA calculations for pickup with $l=2$ using potential sets X and Y, respectively; the calculated maxima have been normalized to the experimental maxima. For an incident energy of 8.0 MeV, there is fair agreement between the calculated curves and the experimental points for the forward angles. However, the position of the experimental minimum in the neighborhood of 110° is not reproduced, and there is disagreement by approximately a factor of 3 between the calculated and observed cross sections at larger angles. The effects of indirect processes are expected to be relatively more pronounced at backward angles, but because the observed cross section is approximately an order of magnitude smaller in this region than in the forward peak, it appears unlikely that these affect the assignment of $l=2$ to the transferred nucleon. At 6.0 MeV, in the region of the largest fluctuations of the excitation functions shown in Fig. 3, the agreement between the calculations and experiment is not as good as that at 8.0 MeV, with neither set of potentials reproducing the structure of the data in Fig. 4; nevertheless, the general slope of the data and forward peaking is reproduced by potential set X. For both He^3 potentials, the agreement of the calculations with the 6.0-MeV α_8 differential cross sections could be markedly improved if the parameters of the alpha-particle potential were allowed to differ from those obtained in fitting the α_9 group.

The $l=2$ assignment to the transferred nucleon is consistent with a $(2s1d)^2$ configuration coupled to $J=2$ outside of a closed O^{16} core, in agreement with the measured spin of this level,[15] and implies that the parity is positive. These are confirmations of the tentative $J^\pi=2^+$ assignment to this level which was suggested as a consequence of the approximate agreement of the excitation energy with the location of the expected analog state of the $T=1$, $J^\pi=2^+$, 1.982-MeV excited state of the O^{18} nucleus.[8] As a check on the calculations, attempts were made to fit the α_8 data with either $l=0$ or $l=1$. Extensive searching with these l values under the previously discussed constraints on the optical-potential parameters failed to yield satisfactory fits.

The 3.133-MeV Level

The alpha-particle differential cross sections corresponding to the population of the 3.133-MeV excited state of F^{18} are shown in Fig. 5. The calculated cross sections shown are for the transfer of an $l=1$ neutron.

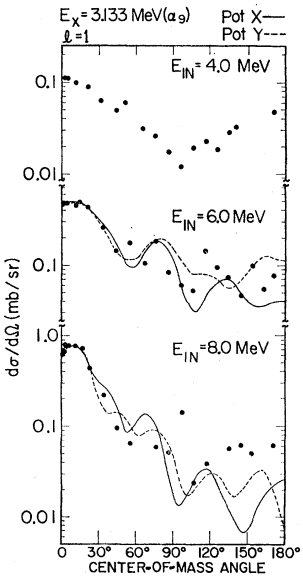

FIG. 5. Measured differential cross sections (dots) for the $F^{19}(He^3,\alpha_9)F^{18}$ reaction at 4.0-, 6.0-, and 8.0-MeV incident energy. The full and dashed curves are zero-range DWBA fits to the data for potential sets X and Y, respectively.

[26] W. T. Pinkston and G. R. Satchler, Nucl. Phys. 72, 641 (1965).
[27] R. Huby and J. L. Hutton, Phys. Letters 19, 660 (1966).

TABLE II. Spectroscopic factors.

Pot.	$E_{in}(He^3)$ E_x (MeV)	6.0 MeV S	8.0 MeV S
X	3.063	0.24	0.24
Y	3.063		0.051
X	3.133	0.33	0.26
Y	3.133	0.066	0.088

As they were for α_8, the calculations were normalized to the peak experimental cross section. Solid and broken curves correspond to potential sets X and Y, respectively. Satisfactory fits were obtained in the forward direction for the angular distributions at both 6.0 and 8.0 MeV. The calculations do not reproduce the experimental maxima near 100°. The results of the calculations obtained with potential set X and with potential set Y are quite similar to each other.

The assignment of $l=1$ to the transferred nucleon corresponds to the 3.133-MeV excited state having negative parity, and is consistent with the state being generated by the $(1p)^{-1}(2s1d)^3$ configuration coupled to $J=1$. This configuration has been employed in calculations which account for a number of the properties of low-lying negative-parity states in the O^{18} nucleus.[3] From these results the presence of similar states in F^{18} may be expected. In a manner similar to that used for α_8, the uniqueness of the $l=1$ assignment for α_9 was tested by attempting to fit the data with $l=0$ or $l=2$. These calculations failed to yield an optical potential which could be successfully employed for both the α_8 and α_9 angular distributions.

Spectroscopic Factors

Spectroscopic factors have been extracted for the two reactions, although their ratio is more reliable than their absolute values. The differential cross section for pickup may be written in the form

$$\frac{d\sigma}{d\Omega}=\frac{2S_b+1}{2S_a+1}\frac{N}{2S+1}\sum_{l,j}\mathcal{S}(l,j)\sigma_{l,j}(\theta),$$

where S_a, S_b, and S are, respectively, the spins of the incoming, outgoing, and transferred particles, $\sigma_{l,j}(\theta)$ is the cross section computed by JULIE, $\mathcal{S}(l,j)$ is the spectroscopic factor including the isobaric spin vector addition coefficient, and N is a normalization constant which includes the strength of the interaction inducing the transition, and, for the (He^3,α) reaction, the overlap of the He^4 wave function with (He^3+n). For the (He^3,α) reaction, the simplest zero-range estimate of N is 6.53, but $N\approx 163\pm 33$ has been obtained empirically in several cases.[14,28] Although more realistic theoretical estimates of N lead to values which are larger than the simplest,[29,30] they are nevertheless smaller than the value 163 which has been utilized in obtaining the results shown in Table II. For potential set X, the spectroscopic factors, which have been obtained from the peak cross sections, are constant to within approximately 25% when considered as a function of bombarding energy. The spectroscopic factor of the 3.063-MeV level for potential set Y is not given because of the lack of agreement between calculations and experimental data at 6.0 MeV previously discussed. On the other hand, at 6.0-MeV potential set X does reproduce experiment for that level for angles less than 30°, and yields consistent results. The values obtained for the 3.133-MeV level are insensitive to the choice of potential set.

The He^3 potential X has the feature of being qualitatively associated with a solution obtained from 9.0-MeV elastic scattering,[20] while potential Y apparently does not have a corresponding solution at that energy. Potential Y gives the best fit to the elastic scattering, but potential X has a broader range of applicability. It is also interesting to note that the exit-channel potential in the potential set X has parameters which are quite similar to those obtained in analyses of the $Ne^{20}(\alpha,\alpha)Ne^{20}$ reaction at[31] 28 and at 18 MeV.[32]

ACKNOWLEDGMENTS

The authors wish to thank Dr. E. H. Auerbach for the use of ABACUS, and Dr. R. M. Drisko for the use of JULIE. They are pleased to acknowledge helpful discussions with Dr. A. R. Knudson. The calculations have been performed at the U. S. National Bureau of Standards Computer Laboratory, Washington, D. C., and at the University of Maryland Computer Science Center.

[28] Cheng-Ming Fou and Robert W. Zurmuhle, Phys. Rev. **140**, B1283 (1965).
[29] R. M. Drisko and R. H. Bassel (unpublished). Referred to by Ref. 14.
[30] G. H. Herling (unpublished).
[31] G. R. Satchler, Nucl. Phys. **70**, 177 (1965).
[32] B. T. Lucas, S. W. Cosper, and O. E. Johnson, Phys. Rev. 144, 972 (1966).